The Journal of Experimental Biology 210, 800-814
Published by The Company of Biologists 2007
doi:10.1242/jeb.000638

Post-natal development of the electromotor system in a pulse gymnotid electric fish

Ana Carolina Pereira[1], Alejo Rodríguez-Cattaneo[1], María E. Castelló[1,2] and Angel A. Caputi[1,*]

[1]*Departmento de Neurociencias Integrativas y Computacionales, Instituto de Investigaciones Biológicas Clemente Estable, Unidad Asociada de la Facultad de Ciencias and* [2]*Departmento de Histología y Embriología, Facultad de Medicina, Universidad de la República, Montevideo, Uruguay*

*Author for correspondence (e-mail: angel@iibce.edu.uy)

Accepted 4 January 2007

Summary

Some fish emit electric fields generated by the coordinated activation of electric organs. Such discharges are used for exploring the environment and for communication. This article deals with the development of the electric organ and its discharge in *Gymnotus*, a pulse genus in which brief discharges are separated by regular silent intervals. It is focused on the anatomo-functional study of fish sized between 10 and 300 mm from the species of *Gymnotus*, in which electrogenic mechanisms are best known. It was shown that: (1) electroreception and electromotor control is present from early larval stages; (2) there is a single electric organ from larval to adult stages; (3) pacemaker rhythmicity becomes similar to that of the adult when the body length becomes greater than 45 mm and (4) there is a consistent developmental profile of the electric organ discharge in which waveform components are added according to a programmed sequence. The analysis of these data allowed us to identify three main periods in post-natal development of electrogenesis: (1) before fish reach 55 mm in length, when maturation of neural structures is the main factor determining a characteristic sequence of changes observed in the discharge timing and waveform; (2) between 55 and 100 mm in length, when peripheral maturation of the effector cells and changes in post-effector mechanisms due to the fish's growth determine minor changes in waveform and the increase in amplitude of the discharge and (3) beyond 100 mm in length, when homothetic growth of the fish body explains the continuous increase in electric power of the discharge.

Key words: electric fish, electric organs, development, *Gymnotus*.

Introduction

Fish of the gymnotiform family (Teleostei) are endowed with specialized electric organs (EO) whose activation generates weakly electric fields (Lissmann, 1958). Both the activation of the EO and the resultant electric field are referred to as the electric organ discharge (EOD).

The electric field serves as a carrier of signals sensed by a mosaic of cutaneous electroreceptors (Bullock et al., 1961). These receptors are well tuned to this carrier, securing its optimal detection and a large signal-to-noise ratio (Bastian, 1986). Thus, the EOD is part of an active sense used for exploring the nearby environment (electrolocation) and for sending messages to con-specific neighbors (electrocommunication). Impedances different from water imprint signals in the self-generated field, in the same way that the voice of a radio presenter imprints signals on the emitted carrier of a broadcasting frequency (Bastian, 1986; Caputi and Budelli, 2006). This allows object detection, location and discrimination. The pattern of repetition of the EOD is itself an electrocommunication signal for conspecifics, in the same way that the sequence of spikes in a neuron codes a message (Black-Cleworth, 1970; Carlson, 2002).

There are two main types of EOs, neurogenic and myogenic. While in neurogenic organs the discharge derives from the synchronic activation of parallel bundles of nerve fibers, in myogenic organs the EOD results from the activation of a population of specialized cells derived from embryonic myogenic tissue, the electrocytes (for reviews, see Bennett, 1971; Baas, 1986; Moller, 1995). The electrogenic system of electric fish with myogenic EO is organized in three main stages: (1) a command signal, generated by a medullary center that triggers each event in the series, (2) spinal and peripheral circuits that organize the spatio-temporal pattern of activation of the EO and (3) the differential excitability of the electrocytes (for reviews, see Dye and Meyer, 1986; Macadar, 1993; Hopkins, 1995; Caputi, 1999; Caputi et al., 2005).

In *Gymnotus*, the multiphasic waveform of the EOD is generated by several neuronal and circuit mechanisms that are responsible for the precisely timed sequential activation of subcellular electrogenic units (the different faces of the electrocytes). Because these mechanisms have been well

characterized in the adult (Caputi et al., 1989; Caputi and Aguilera, 1996; Caputi, 1999), it is now possible to identify a number of stages in the development of the electrogenic system of *Gymnotus*, and this makes it an excellent example for the study of general principles of motor development.

Earlier reports on this topic indicate that the wave gymnotids *Eigenmannia lineata* and *Apteronotus leptorhynchus* (Kirschbaum and Westby, 1975; Kirschbaum, 1977; Kirschbaum, 1983; Kirschbaum and Schugardt, 2002) and the mormyrids (Szabo, 1960; Denizot et al., 1978; Denizot et al., 1982) develop a temporary larval EO that is later substituted by an adult EO. This process is still more conspicuous in the case of Apteronotidae, in which the larval myogenic EO is replaced in the adult by a neurogenic EO that has a different location and electrogenic mechanism (Kirschbaum, 1977).

The development of the EOD in gymnotid pulse species was described more recently in *Brachyhypopomus pinnicaudatus* (Franchina, 1997) and in *Gymnotus carapo* from Trinidad and *Gymnotus mamiraua* from Brazil (Crampton and Hopkins, 2005). In both cases, a progressive maturation of the EOD waveform from larval to juvenile stages was shown. Rather than showing evidence of a larval EO, Franchina's conclusions favor the hypothesis that *B. pinnicaudatus* has a single EO throughout life (Franchina, 1997).

According to the literature, three main periods can be described during fish development: early larval, late larval and juvenile. A single larval stage was considered by Kirschbaum and Schugardt (Kirschbaum and Schugardt, 2002), but two larval stages were defined by Franchina (Franchina, 1997), referring to Blaxter, 1988: early (defined by the endogenous feeding on the yolk) and late (in which the digestive organs, the exogenous feeding and, in electric fish, the EOD appear). Juvenile stages are usually considered as the forms that are essentially similar to the adult except in size and mature gonads (Franchina, 1997).

The present article is focused on late larval and juvenile ontogeny of the electromotor system in the best-studied species of *Gymnotus*, previously identified as *G. carapo* but at present in the process of being described as a different species (see Materials and methods), whose adult EOD is characterized by a sequence of four waveform components (V_1–V_2–V_3–V_4) (Trujillo-Cenóz et al., 1984). Our observations indicate that (1) *Gymnotus* sp. do not exhibit a larval EO different from the adult EO; (2) the mean rate and regularity of the EOD increase with growth, reaching stable values in fish of about 30–40 mm length; (3) EOD complexity increases by the consecutive and consistent addition of the EOD waveform components, according to the sequence V_3–V_4–V_1–V_2, and (4) electrosensory-evoked novelty responses were present in all the specimens studied, indicating the presence of electrolocation.

Materials and methods

This work was performed in specimens captured in the Laguna del Cisne (latitude 35°50′ S, longitude 55°08′ W). The species was formerly identified as *Gymnotus carapo* (Trujillo-Cenóz et al., 1984, following the description of Linneo 1758). Since the literature on gymnotids has been recently revised, two fixed adult specimens were sent to J. Albert (University of Louisiana, USA), who compared them with a collection obtained in the context of a large-scale survey of this genus (http://www.flmnh.ufl.edu/gymnotus) (see also Albert and Crampton, 2001; Albert and Crampton, 2003; Albert and Crampton, 2005) and suggested that this species does not correspond with any formally described species of *Gymnotus*.

We based our study on more than 250 fish found as schools of 8–12 small fish (between 1 and 4 cm in length), usually together with a single adult fish of about 20–25 cm in length. Fish were captured on nine expeditions through the summer seasons of 2004/2005 and 2005/2006. Successive expeditions to the same site allowed us to capture fish in successive stages of development. Linear regression analysis between the date of capture at such a site and fish length indicated that fish length is a good indicator of fish age (r=0.86, N=127). Fish were studied in the laboratory during the two or three days after capture, characterizing the following aspects as a function of fish length: (1) the anatomy of the EO, (2) the head-to-tail waveform of the electric field in water and the EOD emission rhythm and (3) the parameters of the fish body's equivalent electric sources and their distribution along the EO.

Anatomy of the electric organ

Seven fish were used for anatomical studies. All of them were deeply anesthetized with an overdose of pentobarbital before fixation. Five fish (185, 68, 65, 30 and 28 mm in length) were used to evaluate the gross anatomy and electrocyte density along the EO. Fish were fixed by immersion for 24 h in a solution containing 1% paraformaldehyde and 1% glutaraldehyde in phosphate buffer (0.1 mol l^{-1}, pH 7.4). The bodies of a 30 mm larva and a 65 mm juvenile were used to calculate the cross-sectional area of the fish body occupied by the EO. The 30 mm larva was sectioned (300 μm) in the transverse plane. The 68 mm fish was cut into pieces of equal length, and a 300 μm slice was obtained from the rostral face of each piece. For both fish, outlines of the sections and of the EO were drawn from microphotographs, and the relative area occupied by the EO was evaluated using an in-house computer program. In the other three fish (28, 68 and 185 mm), electrocyte density was estimated by counting electrocytes either using transillumination of the whole fish following removal of the skin or in parasagittal sections.

In addition, to study the larval EO, two 12 mm larva were used. One was osmified (1% water solution of OsO_4 for 24 h), dehydrated and included in Araldite™. Horizontal semi-thin sections were counterstained with boracic methylene blue. The other larva was fixed using De Castro's solution and silver impregnated using Cajal's photographic procedure (Ramón y Cajal and De Castro, 1933). The whole body was dehydrated, embedded in Araldite™ and sectioned in the frontal plane (60 μm).

The head-to-tail electric field and its emission pattern

The electric field generated by the EOD was recorded in 179 fish (44 fish captured in the austral summer of 2005 and 135 captured in the austral summer of 2006). We used two pairs of electrodes positioned in the longitudinal axis of the fish: the first pair was positioned with each electrode 0.5 cm away from the extremes of the fish body (i.e. at the head and tail), and the second pair was placed further away, with each electrode 42 cm from the center of the longitudinal axis of the fish body (the electrodes were placed at opposite corners of a 60×60 cm aquarium). In some cases, both recordings were performed simultaneously. We controlled temperature and water conductivity to match the values observed in nature for each fish population (20°C for the fish gathered in the summer season of 2004–2005 and 26°C for the fish gathered in the summer season of 2005–2006, and 350 μS cm^{-1} in both groups). The EOD fields were differentially amplified (×100), band pass filtered (10 Hz–10 kHz), averaged (8 or 64 traces) and digitized at 100 kHz using a digital oscilloscope. Waveforms were analyzed in the time domain by direct inspection and measurement of the peak times and amplitudes for each component and in the frequency domain using a fast Fourier transform protocol.

The head-to-tail EOD recordings were also converted into square pulses using a window discriminator. These pulses triggered a digital switch on the serial port of a computer sampled at 12 kHz, and a series of point processes were constructed from 76 fish (37 from 2005 and 39 from 2006). For each time series of the EODs, we constructed first-order interval rasters and histograms. The parameters of the histograms were calculated in order to assess the mean rate (mean, median interval), the interval variability [variance, coefficient of variation (standard deviation/mean) and Fano factor (variance/mean)] and the symmetry of the variability (skewness). In seven fish of 30, 38, 50, 67, 72, 90 and 110 mm length, we studied the repetition rate (the inverse of the mean interval of EOD trains of 20 s in duration) as a function of water temperature at a water conductivity of 350 μS cm^{-1}.

The electric source equivalent to different regions of the fish body

In order to analyze the activation pattern of the EO, we used the multiple air gap technique described by Caputi et al. (Caputi et al., 1993) in 20 fish (lengths ranging from 30 to 220 mm). To characterize the equivalent electric source of the entire fish, we recorded the EOD between two points, one at the caudal limit of the head and the other at the tip of the tail, while the fish's body was maintained in air. Two resistors of known value were connected in series with the inputs of a recording differential amplifier having very high input resistance (>100 MΩ). While one of these resistors was constant throughout the experiment (1 kΩ or 2.2 kΩ), the other was varied in a controlled manner in order to explore the relationship between the generated voltage and the supplied current. For all of the observed waveform components except the last negative one, the voltage was a linear function of current. In the linear case, the ordinate intersection of the line corresponds to the electromotive force of the equivalent source, the abscissa intersection corresponds to the maximum supplied current, and the slope of the line corresponds to the equivalent internal resistance in series with the electromotive force (Cox and Coates, 1938; Bell et al., 1976; Caputi et al., 1989). In order to show that the mechanism for the generation of V_1 and V_2 is different, we compared the effect of nicotinic blockage on these components in a fish of 65 cm length. In this animal the simple air gap procedure was performed before injecting intraperitoneally 100 μg of d-tubocurarine and just after the fish stopped respiratory movements.

The same procedure allowed us to characterize either the pattern of electromotive force generated by contiguous body regions of 5 mm length, from the tip of the tail to the head, or their serial sum, which corresponds to the equivalent electromotive force generated by the whole body. We recorded the regionally generated voltage while the fish was in air, measured between two electrodes connected to a high-input impedance differential amplifier (×10, band pass 10 Hz–10 kHz). A head-to-tail signal was similarly and simultaneously obtained and used as a time reference to align successive recordings taken from contiguous body regions. To compare fish of different length and different recording regions, we defined an index of electrogeneration for each recorded deflection of the EOD in each region. This index was calculated as the measured electromotive force divided by the length (expressed as a percentage of fish length) of its generating region. The index was then plotted as a function of the position of the center of the generating region, measured as the distance to the jaw and expressed as a percentage of the fish length.

Results

The gross anatomy of the electric organ

The gross anatomical organization of the EO of juveniles and larvae is similar to that of the adult. Approximately 700 electrocytes are serially packed in tubes rostro-caudally parallel to the sagittal plane. Two of the four tubes lying on each side of the midline extend from the pectoral girdle, just rostral to the anal papilla, up to the tip of the tail. The other two, shorter tubes extend from the rostral origin of the anal fin up to the tip of the tail. Thus, at the abdominal region, the EO consists of two pairs of tubes on each side of the midline (Fig. 1A). Each pair of tubes runs on a horizontal plane in the ventral abdominal wall immediately beneath the skin. Between the tubes of each pair it is possible to identify a nerve similar to the anterior electromotor nerve observed in the adult (arrows, Fig. 1A). On the trunk and tail regions, four tubes on each side lie parallel on parasagittal planes (Fig. 1B). Since in larvae the head and the abdominal cavity occupy the rostral 50% of the fish body and the tail region is very thin, the largest part of the EO occupies the central-caudal quarter of the fish body. At this level it can be already observed that the more dorsal tube is larger than the others (Fig. 1B). Caudal electrocytes are very

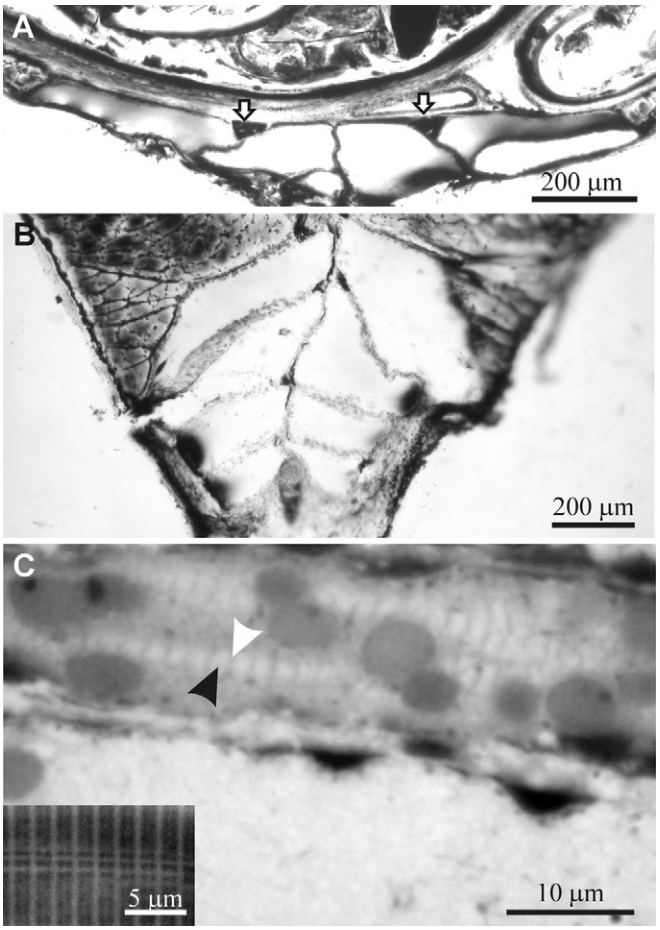

Fig. 1. The electric organ of larval fish. Photomicrographs of coronal sections of 12 mm-long fish impregnated with silver at the abdominal region (A) and the middle region (B) of the fish body. As shown in A, in the abdominal region, the electric organ consists of pairs of tubes on each side of the body midline. A nerve is also evident, cut in cross section, lying at the dorsal edge between the lateral and medial electrocytes on each side (arrows). Thin branches innervating the caudal faces of the electrocytes emerge from these nerves (not shown here), indicating that they correspond to the anterior electromotor nerves observed in the adult. After the emergence of the anal fin, the electric organ consists of two sets of four tubes on each side of the midline (B). Note the dorsal–ventral decrease in the electrocytes' cross-sectional area. (C) Microphotograph of a semi-thin section of a 12 mm-long fish showing parts of two electrocytes. The striated appearance of the cytoplasm of one of them indicates its myogenic origin (black and white arrows point to the clear and dense phases of the stria, respectively). The periodicity of this striation is similar to that of skeletal muscle (inset), although it is much fainter.

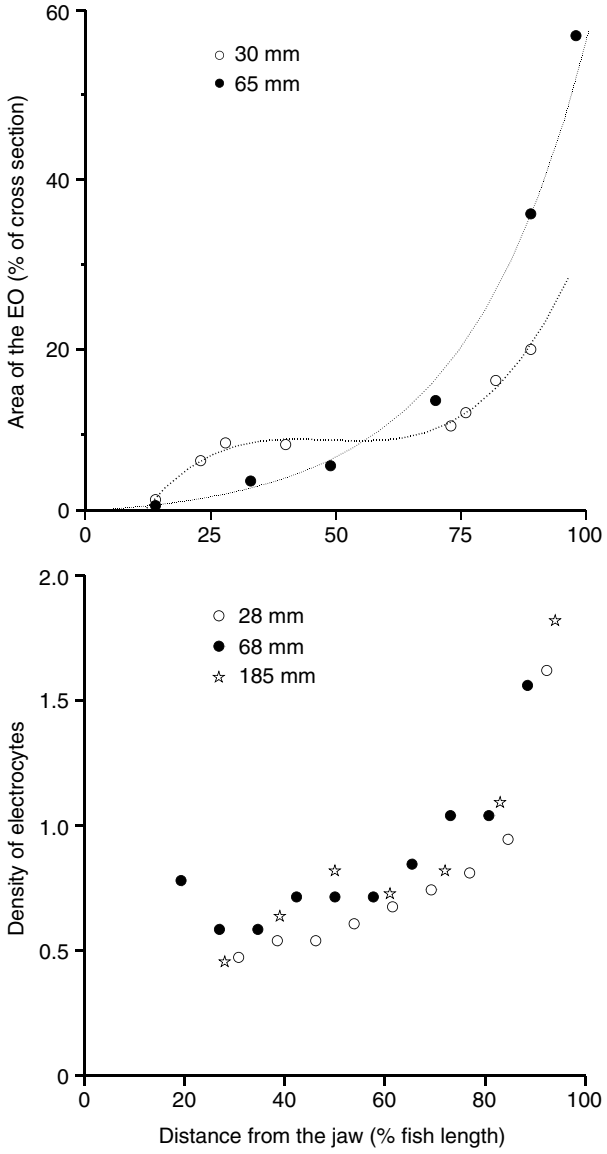

Fig. 2. Development of the electric organ (EO) from larval to adult stages. (A) Area of the fish body occupied by the EO (expressed as a percentage of the cross-sectional area) as a function of the distance from the jaw (expressed as a percentage of the fish length). The area of the fish body occupied by the EO in the rostral half of the fish body is greater in larvae (30 mm) than in juveniles (65 mm), and the contrary holds for the caudal half of the fish body. (B) For all studied fish (28, 68 and 185 mm), the density of electrocytes (expressed as the number of electrocytes per 1% of fish body length) increases from the rostral to the tail regions.

small and show zones with the typical striation of sarcomeric proteins (Fig. 1C).

Although the anatomical organization of the EO is similar, the area that the EO takes up within the body cross-section, and its distribution along the body, differs in larvae, juveniles and adults. The area of the EO is a larger fraction of the total cross-sectional area at the center of the fish body in larvae than in juveniles, while the area occupied by the EO at the caudal region of the fish is larger in juveniles than in larvae (Fig. 2A). The electrocyte count shows a similar density profile, increasing exponentially along the rostral–caudal axis (Fig. 2B).

The rhythm of EOD series

Young fish ranging from 12 to 100 mm emit very regular EODs, which were evaluated by rasters (Fig. 3A) and their corresponding first-order interval histograms (Fig. 3B).

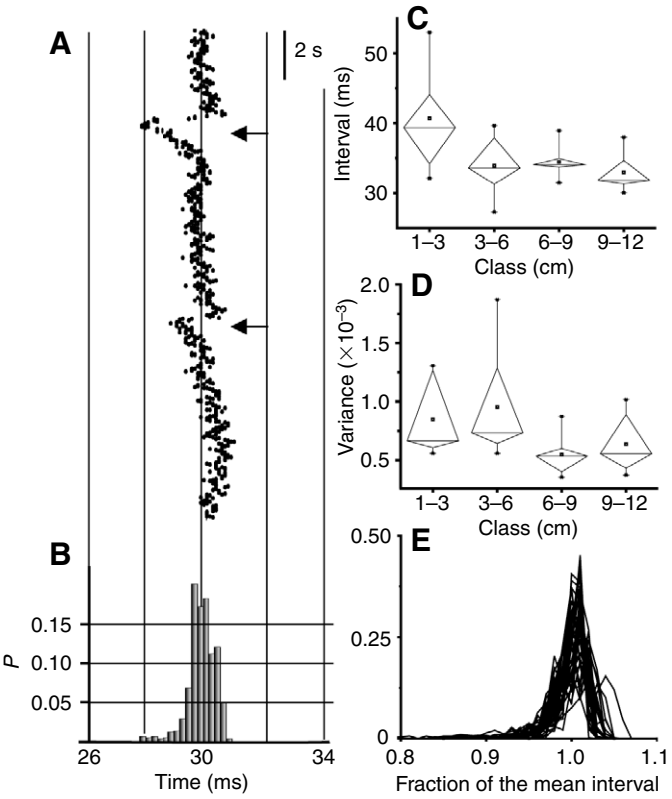

Fig. 3. Characteristics of the pacemaker frequency as a function of fish length. (A) Raster of the first-order intervals emitted by a resting fish of 37 mm length. Note the regularity of electric organ discharge (EOD) interval, interrupted by accelerations, followed by slower relaxations up to the basal EOD interval (arrows). (B) Histogram of the inter-EOD intervals represented in A. Note the skew of the histogram that results from the accelerations indicated by the arrows in A. (C) Box plot comparing the individual means of the EOD intervals exhibited by fish of different lengths. The first category, fish shorter than 30 mm, discharged their EO at a rate significantly lower than the others. (D) Box plot comparing the variance of the EOD intervals exhibited by fish of different lengths. The EOD was significantly more regular for the two categories above 60 mm. (E) First-order frequency polygon of the inter-EOD interval normalized to the mean interval obtained from 45 fish ranging from 12 to 226 mm, showing the constancy of the distribution.

Fish shorter than 30 mm discharged their EO at a rate significantly lower than fish longer than 30 mm (Fig. 3C) (statistics for 41 fish gathered in 2005 studied at 20°C; Kruskal-Wallis ANOVA test, $P<0.05$; Wilcoxon test between the category of fish below 30 mm and each of the other categories of Fig. 3C indicated significant differences, $P<0.05$ in each comparison). Similar results were obtained for fish captured in 2006. However, since the range of length was narrower, we compared fish below and above 45 mm length (Wilcoxon test, $P<0.05$, $N=35$).

In addition, the interval was more variable below 60 mm than above this length. The interval variability was evaluated by its variance (Fig. 3D), coefficient of variation and Fano factor (variance divided by the mean). For all these parameters, we found significant differences between the categories shown in Fig. 3D (Kruskal-Wallis ANOVA test, $P<0.02$, d.f.=3, 20°C, fish gathered in 2005). Further comparison between categories yields significant differences for the following pairs: 10–30 mm *vs* 60–90 mm, 10–30 mm *vs* 90–120 mm, 30–60 mm *vs* 60–90 mm, and 30–60 mm *vs* 90–120 mm, (Wilcoxon test, $P<0.05$). For fish gathered in 2006, there was a significant difference between categories defined as below and above 45 mm (Wilcoxon test, $P<0.05$, $N=35$).

Pacemaker rate was linearly dependent on temperature (studied range, 17–31°C). Interestingly, the slope of the line was similar for all studied stages, suggesting a similar degree of pacemaker sensitivity to temperature (Fig. 4).

The shape of first-order frequency polygons of the inter-EOD interval normalized to the mean interval was similar at all developmental stages (Fig. 3E). Even in the absence of any sensory stimuli noticeable to the human observer, there was always a negative skew reflecting the occurrence of brief, abrupt decreases of the inter-EOD interval (i.e. accelerations) followed by a relaxation curve. These sudden acceleration–relaxation patterns (arrows in raster of Fig. 3A) were of variable amplitude, reaching up to 10–15% of the basal interval. The largest accelerations were triggered by novel sensory stimuli of various sensory modalities, very similar to the so-called 'novelty responses' described by Lissmann (Lissmann, 1958) (see also Bennett and Grundfest, 1959; Szabo and Fessard, 1965; Larimer and Macdonald, 1968; Bullock, 1969; Heiligenberg, 1980; Meyer, 1982; Schuster and Otto, 2002; Caputi et al., 2003).

Particularly significant are the novelty responses caused by a short circuit close to the snout, indicating that the electrosensory system is functional even in the smallest recorded fish (Fig. 5A). Novelty responses of larvae are characteristically of higher amplitude (compare profiles in Fig. 5A and Fig. 5B, and see plot in Fig. 5C; Wilcoxon test, $N=21$, $P<0.05$) and longer duration than those displayed by juvenile and adults (the half relaxation time was significantly longer in fish shorter than 45 mm than in fish longer than 45 mm; Wilcoxon test, $N=21$, $P<0.05$, compare profiles in Fig. 5A and Fig. 5B and see plot in Fig. 5D).

The electric field generated by the EOD in water

We found that recordings obtained with the electrodes placed along the body axis more than 20 cm away from the fish were more reliable and reproducible for evaluating the EOD temporal waveform (Fig. 6A) than those located near the body surface. Therefore, far-field measurements were used in the following quantitative analysis. In order to have an index of the EOD amplitude independent of its waveform, we calculated the root mean square value of the EOD associated field (rmsEOD) from 10 ms oscilloscope traces (sampling frequency 100 kHz, water conductivity 350 $\mu S\ cm^{-1}$). As shown in Fig. 6B, the rmsEOD increased linearly with the square of the fish's length ($r=0.91$, $N=104$, $P<0.01$). It is important to note that this increase in the rmsEOD, indicating that the delivered power

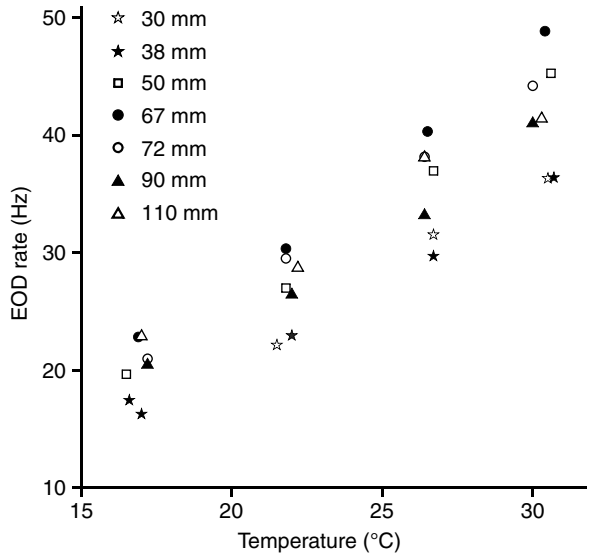

Fig. 4. Electric organ discharge (EOD) rate as a function of water temperature comparing larvae and juveniles of different length, gathered in the same day. Note that in all specimens there is a linear relationship with similar slope and that the smaller fish have a lower rate.

increases with fish length, occurred not only during development but also in adults, and probably throughout the whole of the fish's life (see Knudsen, 1974; Aguilera et al., 2001).

As a global index of the EOD waveform, we used the frequency at the peak of the power spectra of the far-field recordings. While the monotonic increase in amplitude appears to reflect the growth of the fish (Fig. 6B), the index of the waveform increases as a function of fish length up to 60 mm in length (Fig. 6C). These results indicate a maturation of the EO and its activation mechanisms during larval and juvenile stages. The shift of the power spectra to the higher frequency range reflects the addition of EOD waveform components in the course of postnatal development (Fig. 6A) until the waveform becomes similar to that of the adult (V_1–V_2–V_3–V_4) (Trujillo-Cenóz et al., 1984).

Our observations using this technique match those of Crampton and Hopkins (Crampton and Hopkins, 2005) in other species. The mono- and biphasic waveforms were found in the presumably youngest individuals (length between 12 and 30 mm). In all cases, the head-positive component (V_3) is the principal one, which is sometimes followed by a small head-negative component (V_4), as exemplified by the recordings obtained from an 18 mm fish (Fig. 6A, biphasic larval stage). Fish between 30 and 45 mm length showed a tri-phasic waveform, including a first head-negative, slow, asymmetric wave (V_1) followed by the positive–negative sequence observed in the previous stage. Note that V_4 was relatively larger than in the previous stage (Fig. 6A, triphasic larval stage). In fish longer than 45–50 mm, the four EOD waveform components present in the adult were clearly identifiable, as well as the notch in the rising phase of V_3 that is characteristic of this species (arrow in Fig. 6A, juvenile). Within a given stage, the relative amplitude of the different waveform components changes gradually.

The fish body as an equivalent source

The adult EOD exhibits four waveform components, V_1, V_2, V_3 and V_4, corresponding to the sequential activation of different regions of the EO by different mechanisms (Caputi et al., 1989). The spatial origin of these waves and their generating mechanisms can be inferred by studying the electric equivalent sources for different regions of the fish body.

The characteristic parameters of the equivalent source of the whole fish body were investigated by measuring the drop of voltage across a variable resistor and the corresponding current flowing through the same resistor (Cox and Coates, 1938; Caputi et al., 1989). The comparison of normalized traces obtained when using a very high resistance (1 MΩ) (Fig. 7A, red) and obtained when using a very low resistance (1 kΩ) (Fig. 7A, black) shows that the waveforms are identical except for the late head-negative component (note that black traces are shown slightly shifted to the right to allow visualization of both waveforms).

Voltage *vs* current plots of the peak of V_3 show a linear relationship in which the ordinate corresponds to the body equivalent electric source, and the slope corresponds to the body equivalent internal resistance (Fig. 7B). The electromotive force for the head-positive component increases as a function of fish length, from 28 to 100 mm (Fig. 7C). For longer fish, the equivalent electromotive force of V_3 stabilizes between 2 and 3 V and the equivalent internal resistance decays as shown by the change of the slope (Fig. 7B).

A linear relationship between current and voltage also holds for the earlier negative waves (V_1 and V_2; data not shown) but not for V_4. Departure from the linear relationship caused by unloading the fish's equivalent electric source is larger for smaller fish. In fact, the relative size of V_4 (ratio V_4/V_3) increased when the fish body was loaded with a very low resistance between head and tail. This increment in the ratio V_4/V_3 decreases as a function of body length (Fig. 7D), suggesting that the generating mechanism of V_4 (action potential propagation from caudal to rostral faces of the electrocytes) increases in efficiency during development.

In fish longer that 20 mm, the analysis of the different regions of the EO was made using the multiple air gap method (Caputi et al., 1993). This revealed the spatial origin of the waveform components of the EOD as shown in Fig. 8, where typical EOD regional waveforms obtained from fish of 30, 47 and 68 mm length are compared. It should be noted that (1) the electrogenerating region (as a percentage of fish body) is shorter and situated more caudally in animals of 30 and 47 mm than in the juvenile of 68 mm length, (2) the duration of the EOD decreases with body length and (3) there is a relative increase in the negative waves with body length.

In order to make a quantitative comparison of the contribution of different regions of the EO to the generation of

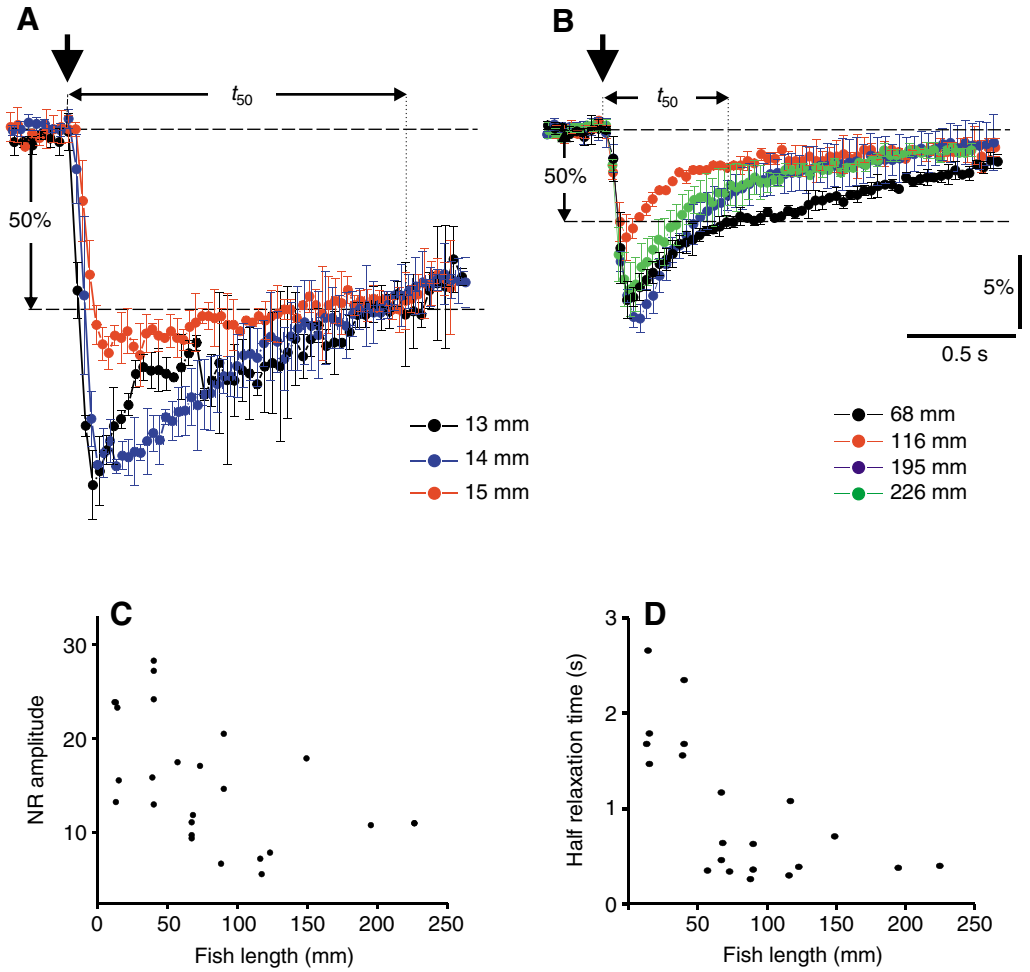

Fig. 5. Novelty responses elicited by electrosensory stimuli. (A,B) Mean ± s.d. (N=10) of the inter-EOD (electric organ discharge) interval normalized to basal EOD interval (upper dashed line=100%), plotted as a function of time. The arrows indicate the moment when two wires are short circuited in front of the fovea. (A) Biphasic larvae exhibit larger and longer-lasting accelerations than (B) juveniles and adults in response to changes in reafferent signals. (C) The amplitude of the novelty response (defined as the maximum shortening of the inter-EOD interval as a percentage of the basal interval) decreases with fish length. (D) The half relaxation time (defined as the time in which the interval returns to values equal to basal minus 50% of the amplitude of the response) also decreases with fish length.

each component at each developmental stage, we studied the strength of the electromotive force generators for each of the waveform components as a function of their position along the fish body. Since we used an air gap resolution of 5 mm in fish of different length, each segment represented a different percentage of body length. Thus, to compare the data from fish of different lengths, we calculated an electrogenic index: the electromotive force divided by the length of the generating region (the latter being expressed as a percentage of the whole fish length).

In Fig. 9, the electrogenic index of the early negative deflection is plotted as a function of the distance from the center of the gap (generating region) to the jaw (expressed as a percentage of fish length). The different panels correspond to fish at different developmental stages. The generator for this deflection in fish below 39 mm was mainly localized in the abdominal region. Note that when fish grow, the head becomes relatively smaller and, consequently, the abdominal region, as well as the regions generating the early negative component, shift rostrally (compare Fig. 9A with 9B). In fish longer than 45 mm, a caudal component appears in the early negative wave (Fig. 9C), which grows with length, generating a bimodal distribution in fish longer than 56 mm (Fig. 9D). In addition, when the fish is partially curarized, the late caudal component of the early negative deflection is more affected than the earlier rostral one (Fig. 10). This indicates that the caudally generated early negative wave component (dark gray box, Fig. 9D) is generated by a membrane process more sensitive to curarization than the rostrally generated early negative wave component (light gray box, Fig. 9D), revealing a different generation mechanism. Therefore, above 55 mm, the presence of both components of the early negative wave (one abdominal, corresponding to the adult V_1, and the other at the trunk, corresponding to the adult V_2) indicates that the

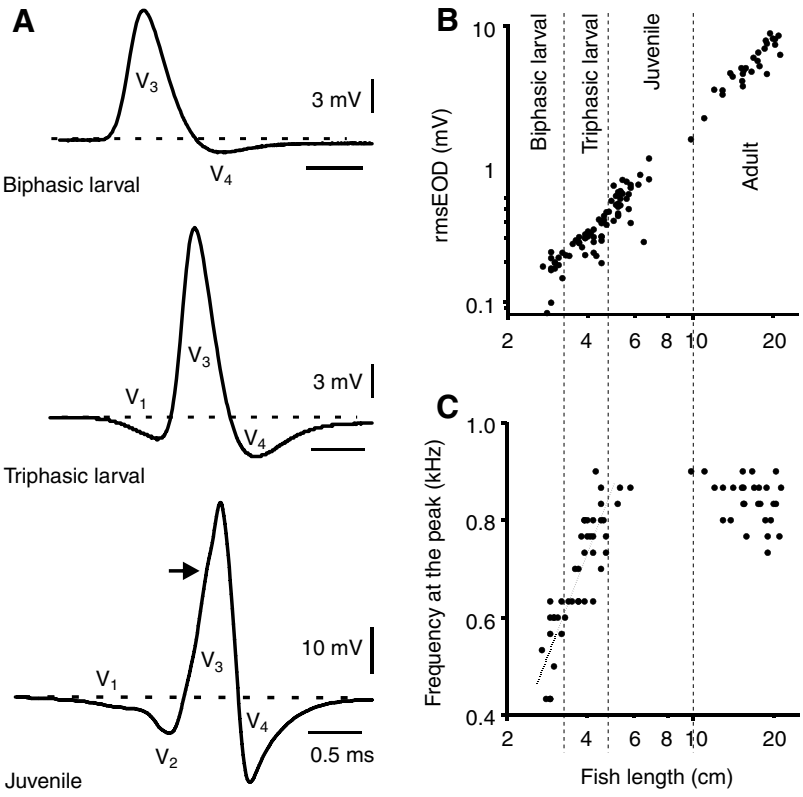

Fig. 6. The electric field generated by the electric organ discharge (EOD). (A) Typical EOD waveforms corresponding to biphasic larval, triphasic larval and juvenile stages, showing the progressive incorporation of EOD components. (B) The root mean square value of the EOD associated field (rmsEOD) is a linear function of the square of the fish length. This relationship holds for larvae, juveniles and adults, in spite of the differences in EOD waveform. (C) During the larval and juvenile stages, the frequency at which the power spectrum of the EOD peaks, increases with fish length.

maturation of the neural mechanisms for the coordination of the neurally activated waveform components of the EOD is complete.

A similar analysis performed for V_3 and V_4 shows that the spatial pattern of their electrogenic sources also depends on body length. In small fish (below 30 mm in length), V_3 increases between 40 and 80% of the fish length (measured from the jaw) (Fig. 11A), stabilizing at the caudal region of the tail. In these fish, V_4 may or may not be present. This is consistent with the poor development of EO at the tail region in this stage (Figs 1C, 2A). For fish longer than 34 mm, the V_3 index grows exponentially with the position of the generator (Fig. 11Aii–iv), which is consistent with the profile of electrocyte density along the EO (Fig. 2B). Nevertheless, some fish show a deviation of the exponential fit at the very tip of the tail. In fish longer than 34 mm, V_4 is generated caudally to 50% of the fish length, and the growth coefficients are larger than those for V_3.

The growth coefficient of V_3 and V_4 in juveniles longer than 55 cm is similar to those of adult fish (Fig. 11Aiv) (Caputi et al., 1989). However, the equivalent electromotive force of the whole body keeps increasing during development until fish reach about 100 mm in length. In addition, the quotient V_4/V_3 increases with body length (Fig. 7B,C). These data on electromotive force and the relatively smaller increase of V_4 as a function of body length when the EO is loaded (Fig. 7A,D) suggest a progressive increase in the electrocytic membrane excitability and EOD power through development.

Discussion

In this paper, we describe the postnatal organization of the electromotor output and some of its structural basis in a *Gymnotus carapo*-like species. This species is not formally described yet (J. S. Albert and W. G. R. Crampton, personal communication). Nevertheless, the occurrence of a single species of *Gymnotus* in Laguna del Cisne indicates that this is the species in which the EOD pattern was described (Caputi et al., 1993). According to Franchina's definition of postnatal developmental stages (Franchina, 1997), our study, including fish longer than 10 mm, only comprises late larval and juvenile stages. We were not able to capture fish shorter than 10 mm in the natural habitat, perhaps because of the capturing method based on detection of electrical activity. According to the data of Kirschbaum and Schugardt, the early larvae lack an EOD and would not be detectable in the natural habitat by probing for the EOD (Kirschbaum and Schugardt, 2002). Besides, as *G. carapo* mouthbreed, the probability of capturing larvae below 10 mm is reduced (Kirschbaum and Schugardt, 2002).

Taking into account the EOD waveform, the late larval stage of *Gymnotus* can be subdivided according to the progressive appearance of the different waves composing the adult EOD: monophasic, biphasic and triphasic late larval stages (Crampton and Hopkins, 2005). In agreement with these observations, we found similar larval stages and an adult-like tetraphasic EOD appearing in juveniles of about 50 mm. This is interesting since these three *Gymnotus* species show, during development, the waveform patterns of EODs exhibited by various gymnotid species at the adult stage. This agrees with

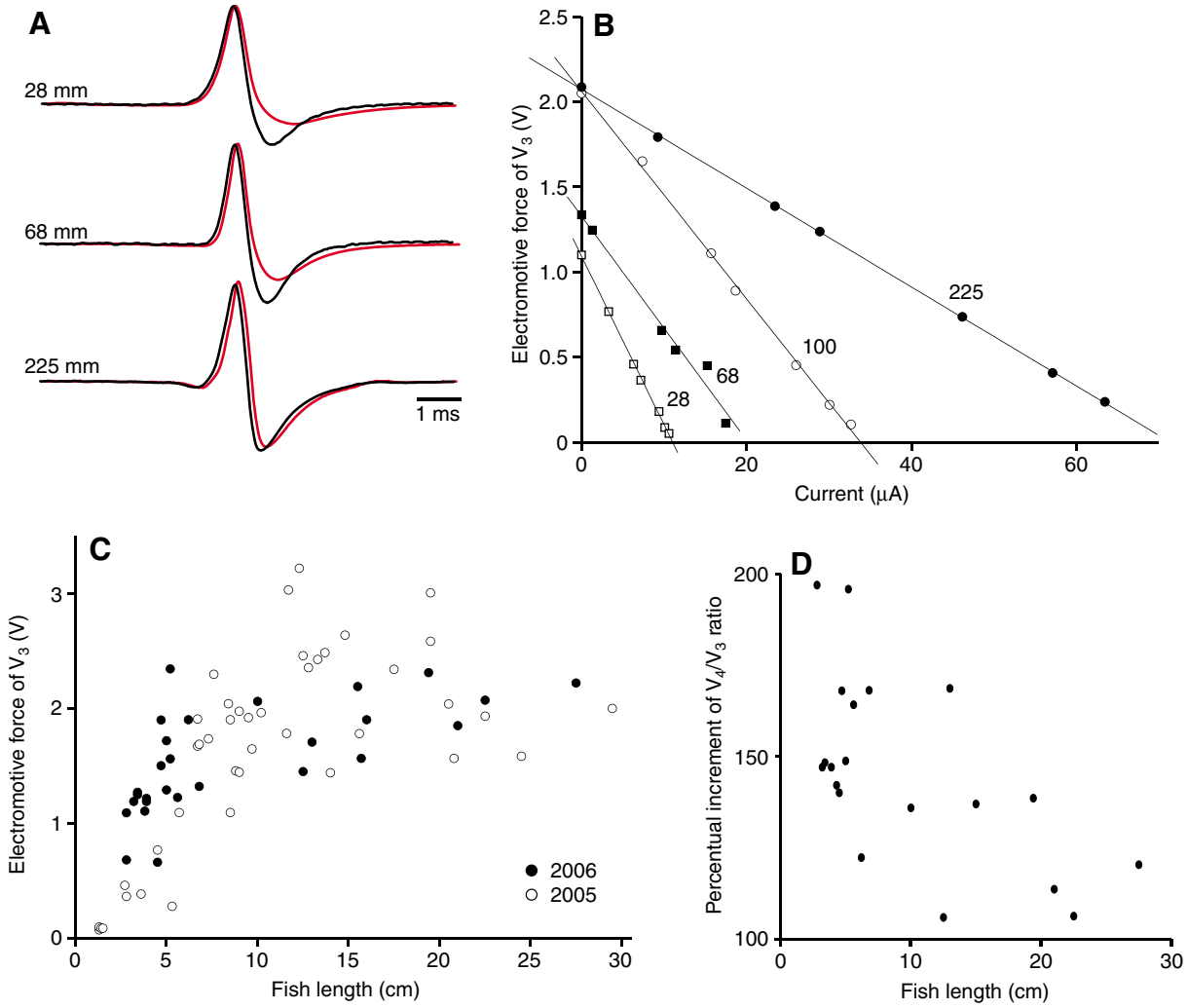

Fig. 7. Development of the electromotive force of the fish's body. The equivalent source was characterized with the air gap procedure (Cox and Coates, 1938; Caputi et al., 1989) by maintaining the fish body out of the water and measuring the drop of voltage across a known resistor. (A) Waveforms obtained using load resistors of 100 MΩ (red) and 1 kΩ (black). All waves except V_4 show a similar time course (note that waveforms are shown slightly shifted in time for the sake of clarity). (B) Characteristic curves of the equivalent electromotive force of the whole fish body for V_3 in a larvae (28 mm), a juvenile (68 mm) and two adults of different length (100 and 225 mm). (C) The electromotive force at the peak of V_3 plotted as a function of fish length. Two populations gathered in consecutive summers are compared. (D) As observed in A, V_4 is modified by an external load on the electric source in the larva and the juvenile but not in the adult. We characterized this phenomenon by the increment of the ratio V_4/V_3 caused by changing the load from 1 MΩ to 1 kΩ. The plot in D shows that this parameter is negatively correlated with fish length (r^2=0.005, N=20), suggesting that maturation is a factor involved in this phenomenon.

the hypothesis that species phenotype reflects the complexity of organization achieved during ontogeny.

In this study, we addressed the following questions: (1) is there a single EO throughout life or, as in other species, is there a larval organ; (2) does the timing pattern of the discharges change through post-natal life; and (3) how does the complexity in the emitted waveform progress through the fish's life?

Anatomical data indicate that the electrogenic larvae possess an EO similar to that of the adult. Our observation of well-organized striations at the more caudal region of the EO contrasts with its absence at the rostral regions, suggesting that there is a rostro-caudal progress of EO development. The finding of striations in electrocytes was reported previously (Baillet-Derbin, 1978; Srivastava and Baillet-Derbin, 1973; Srivastava and Szabo, 1972; Denizot et al., 1982), even in adults, indicating the myogenic origin of electrocytes. In addition, the reappearance of sarcomeric structures after nerve section (Zakon et al., 1999; Zakon and Ungez, 1999) indicates the role of electromotor neuron innervation on the induction of mature electrocyte features.

Functional data indicate that the EO, the mechanisms coordinating its timing of activation and the emitted waveform have a characteristic sequence of maturation during post-natal development, as summarized in Fig. 12.

Behavioral data indicate that electroreception was present in

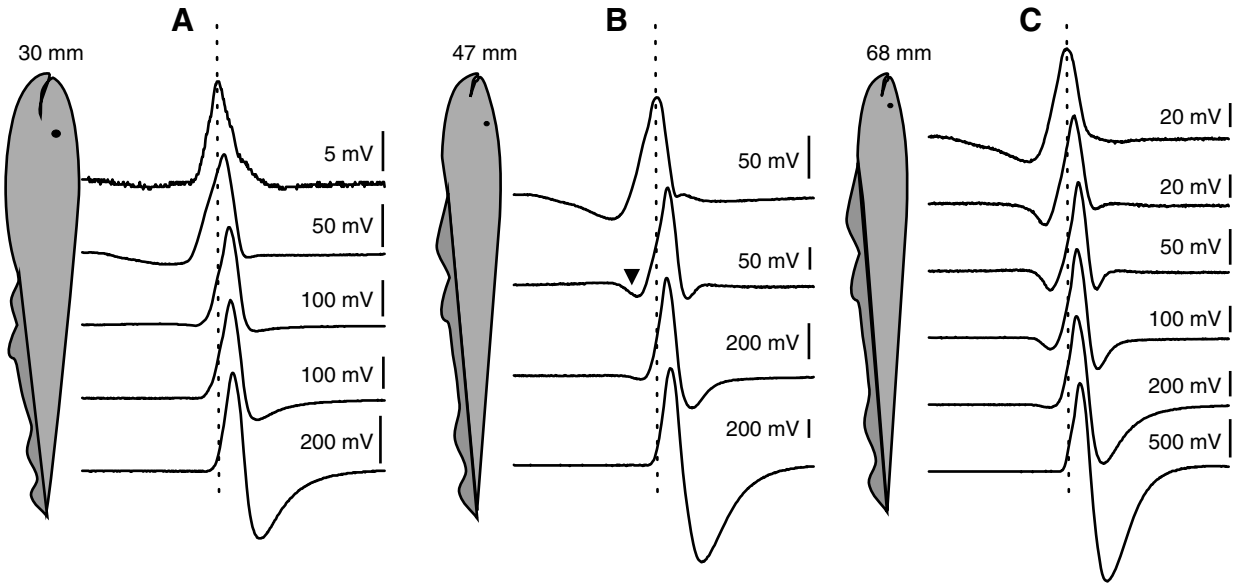

Fig. 8. The spatio-temporal pattern of the equivalent electromotive force along development was studied using the multiple air gap technique [a procedure that allowed the identification of the generation site of the different waveform components of the electric organ discharge (EOD) (Caputi et al., 1993)]. (A) The 30 mm fish exhibited a three-phase EOD with a slow early negative component generated at the abdominal region, a positive component generated all along the body, and a late negative component generated at the tail region. (B) The last component to appear (V_2) was clearly identified in the fish of 47 mm length (second trace, arrowhead) and was completely developed in (C) the juvenile of 68 mm length. Note the progressive reduction of the EOD duration and the relative increase of the late negative component (V_4).

the smallest larvae captured, since they responded with novelty responses to impedance changes in their close environment. Since in late larvae, the EOD and electroreception are present, we presume that there is also active electroreception. However, in our experimental condition, we are not able to rule out possible artefactual currents that might be produced when switching the short circuit activating those ampullary electroreceptors insensitive to the EOD.

In order to guide the discussion concerning the ontogeny of the EO and the EOD waveform, we believe that it is important to analyze our findings in the context of the present hypotheses on the organization of the electromotor–electrogenic system of pulse gymnotids, as described briefly below (Caputi, 1999) (Fig. 12A).

The organization of the electromotor–electrogenic system

The electromotor system has two functional compartments: (1) a pacemaker nucleus setting the timing of the EOD and (2) a pattern generator setting the EOD waveform. The link between these subsystems is a relay nucleus located in the medulla. The pacemaker nucleus receives higher control from sensory systems and motor collaterals and projects to the relay nucleus, which in turn sends descending projections to the spinal electromotor neurons. Two types of electromotor neurons innervate rostral and caudal faces of the electrocytes (Lorenzo et al., 1988; Trujillo-Cenóz et al., 1986; Caputi and Trujillo-Cenóz, 1994). By means of a precise combination of spinal and peripheral delay lines, the nervous system achieves the coordination of a complex EOD waveform with a submillisecond precision (Caputi et al., 1993; Caputi and Aguilera, 1996).

The EOD waveform consists of four components that (1) occur in a stereotyped temporal sequence (V_1 to V_4) (Trujillo-Cenóz et al., 1984), (2) have different electric generators characterized by their electrogenic parameters and location along the EO and (3) have different subcellular generating mechanisms. The EO of the adult consists of four tubes of electrocytes on each side, aligned parallel on parasagittal planes (Trujillo-Cenóz et al., 1984). While the rostral 70% of the dorsal tube contains doubly innervated electrocytes (receiving synaptic contacts on their rostral and caudal faces), the electrocytes in the other tubes are innervated only on their caudal faces (Szabo, 1960; Trujillo-Cenóz and Echagüe, 1989). Following Paccini's principle (Keynes et al., 1961), head-positive deflections are due to the activation of caudal faces, and head-negative deflections are due to the activation of rostral faces. Thus, the activation of the caudal faces of most of the electrocytes serves to generate the head-positive wave V_3, while the further richness and complexity of the EOD waveform is due to the timed activation of rostral faces of the anterior 70% of the dorsal tube. V_1 is generated by the subthreshold activity of the rostral faces of doubly innervated abdominal electrocytes (Lorenzo et al., 1988), V_2 is originated in the action potentials neurally generated at the rostral faces of double innervated electrocytes of the main body region (Bennett and Grundfest, 1959; Macadar et al., 1989) and V_4 is generated by action potentials at rostral faces of caudally innervated electrocytes, resulting from propagation of the

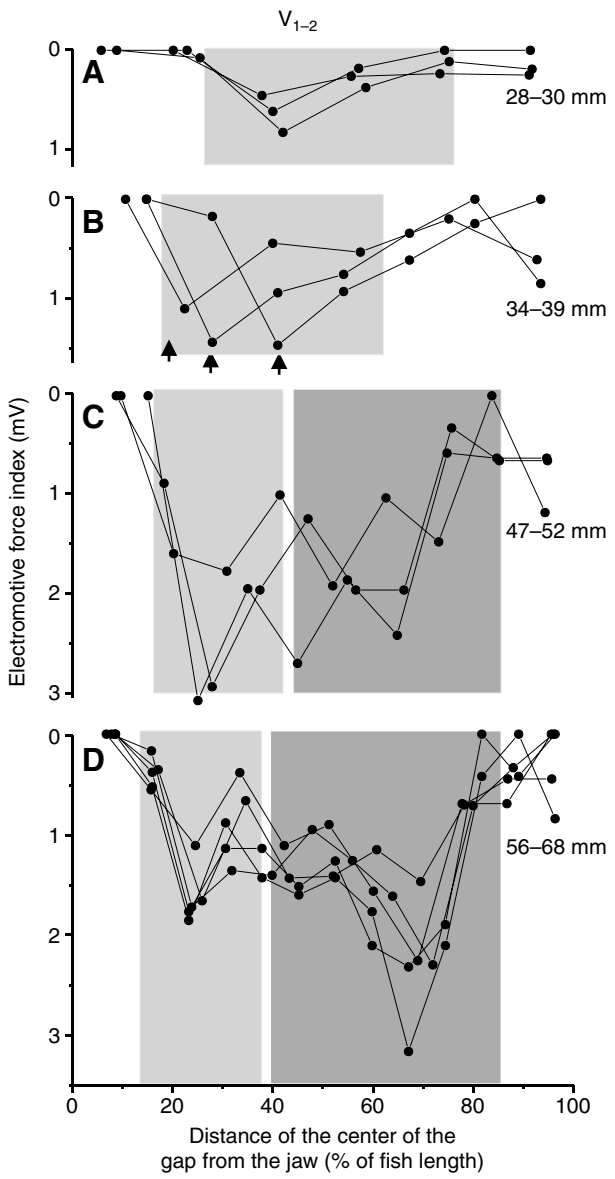

Fig. 9. Regional contribution of the fish body to the electromotive force during development. The contribution of regions corresponding to 1% of the fish length was estimated by plotting the regional electromotive force normalized by the length of the fish region in which it is generated (electromotive force per 1% of fish length) as a function of the position of the center of the region along the fish body (distance from the jaw expressed as percentage of fish length). The early negativity shows two components of different spatial origin and maturation times. In larvae (A,B), the generated electromotive force is largest at the rostral portions of the generating electric organs and shows a slow decay as a function of the distance from the jaw. Note that the peak of the curve moves rostrally as the fish grows (arrows in B). This coincides with the smooth wave observed in time-based recordings and therefore should be classified as V_1 (light gray box). (C) A second component appears in juveniles of about 47–52 mm length and (D) is clearly defined beyond 55 mm of fish length. This component corresponds to the fast component generated at the center of the fish body, V_2 (dark gray box).

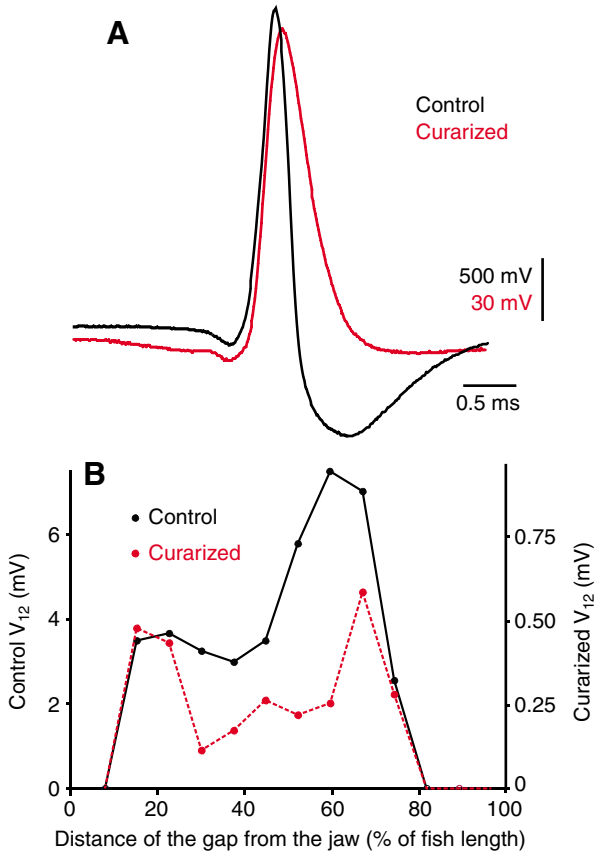

Fig. 10. Further evidence of the different mechanisms of generation of V_1 and V_2 can be obtained by fish curarization, which blocks transmission at the neuro-electrocyte junction. The dose was adjusted to be just enough to stop breathing but not enough to completely block the discharge. (A) The head-to-tail equivalent electromotive force of a fish in control (black) and curarized (red) conditions. (B) The spatial profile of the first negative deflection in control (black) and curarized (red) conditions. Note the differential effect on V_1 and V_2; V_1 is the less affected component because it is generated by the subthreshold activation of the rostral membranes of doubly innervated electrocytes. V_4 is absent because the amount of current generated by V_3 is subthreshold for generating an action potential at the rostral faces of single innervated electrocytes.

action potentials from the caudal faces (Bennett and Grundfest, 1959; Caputi et al., 1989).

Development of the pacemaker and its control system

The main mechanisms of membrane oscillation of pacemaker neurons appear to be fully mature in the late larvae because of the regularity of the inter-EOD interval. Further evidence for this assertion is the similar sensitivity to temperature exhibited by fish of different lengths. It is likely that the same oscillatory mechanism is present in larvae, juveniles and adults, since the slope of the line relating EOD rate and temperature is the same (Fig. 4D).

The negative skew of the first-order histogram of inter-EOD intervals indicates the effect of sensory inputs on the command

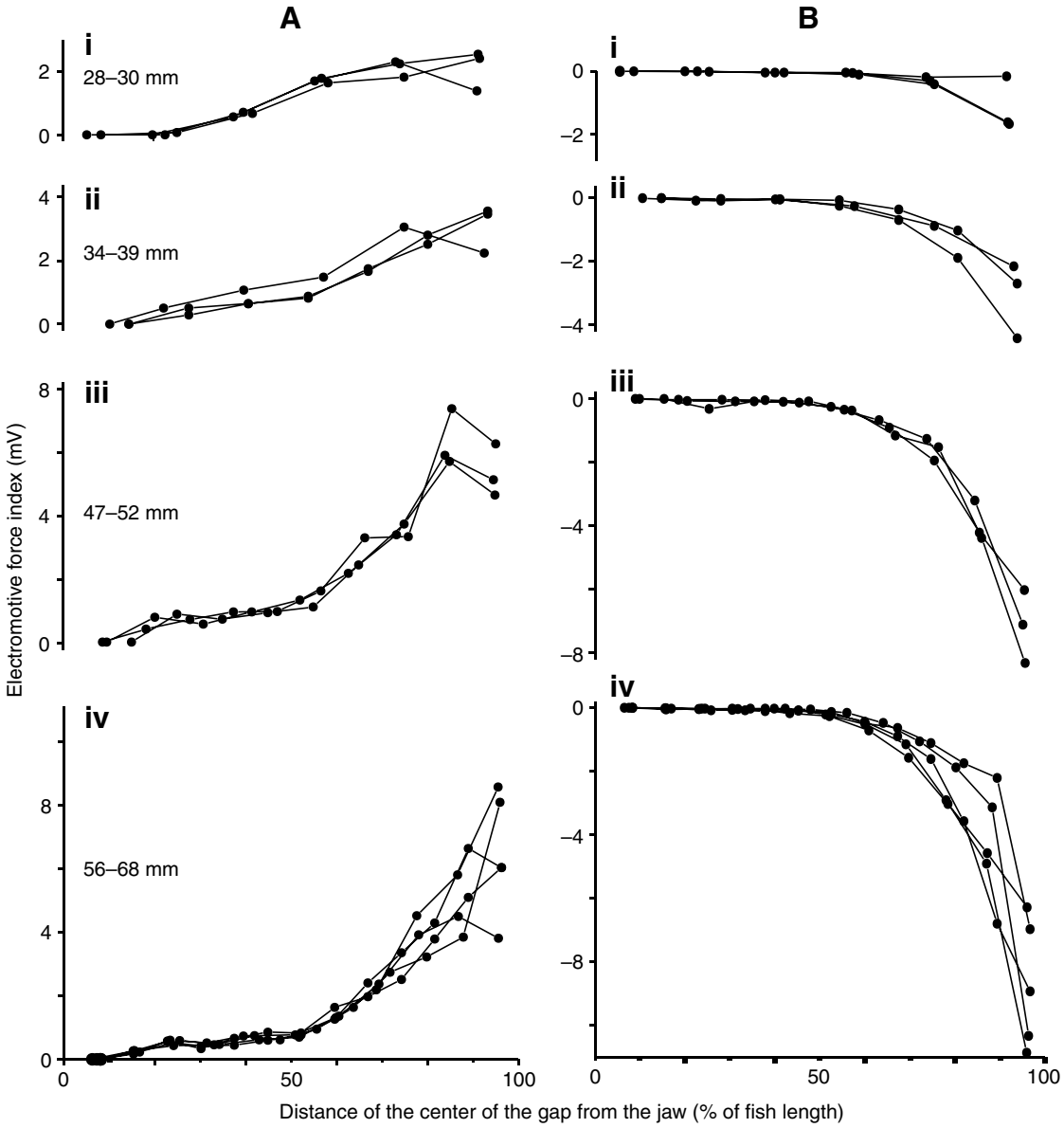

Fig. 11. Development of (A) V_3 and (B) V_4. To compare the data from fish of different length (i–iv), we calculated an electrogenic index: the electromotive force divided by the length (expressed as a percentage of the fish length) of the generating region. In all fish, there is a head-to-tail progressive increment of the electrogenic index with percentage of fish length. Note that both the maximum amplitude and the slope of the curves of both waveform components increase as fish grow. The increase of the growth coefficient for V_4 is larger than for V_3.

nucleus and suggests that both young and adult fish EODs are driven by a regular pacemaker controlled by descending inputs with mainly an accelerating effect. However, the statistical parameters of the inter-EOD histogram suggest that the pre-pacemaker control systems continue developing until the very early juvenile stage. In fact, the basal rate of the pacemaker is significantly lower in the smaller larvae (i.e. shorter than 30 mm) and the pacemaker variability is larger in larvae than in juveniles.

The maturation of the sensorimotor control of pacemaker discharge within the larval period is also shown by the development of innate behaviors such as novelty and jamming avoidance responses (JAR). We found that fish below 45 mm display novelty responses of larger amplitude and longer relaxation phase than those displayed by juveniles and adults (Fig. 5). Consistently, in the wave fish *Eigenmannia*, the JAR appear in specimens between 12 and 15 mm length, strengthening with maturity until they approach adult values at about 45 mm length (Hagedorn et al., 1988; Hagedorn et al., 1992; Viete and Heiligenberg, 1991). The postnatal maturation of the electrosensory–electromotor cycle contrasts with the development of the startle response demonstrated in non-electric teleosts (*Danio rerio*, 40 h after fertilization) (Eaton et al., 1977). In electric fish, Mauthner cell activation evokes

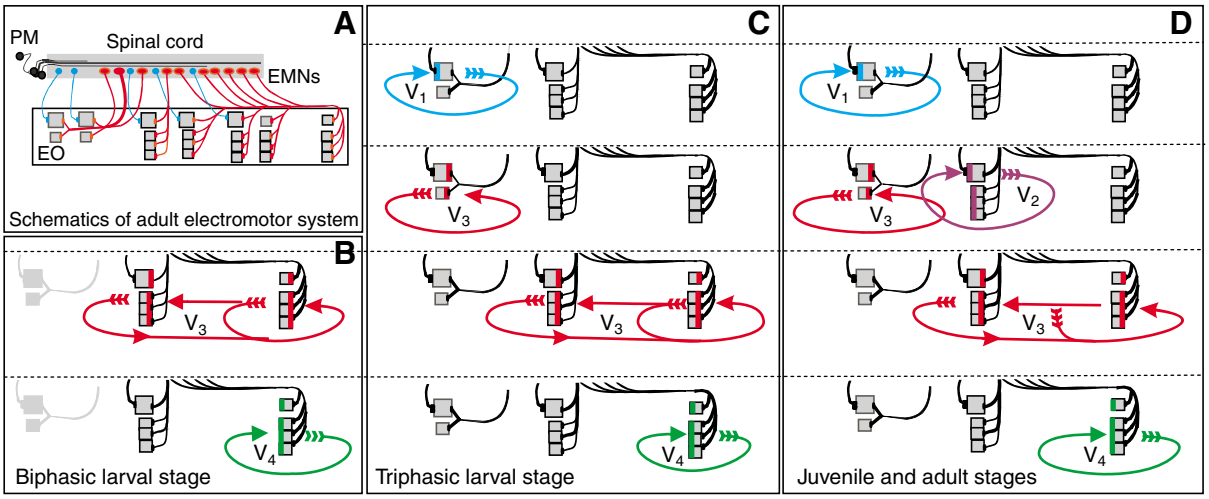

Fig. 12. (A) Schematics of the electrogenic system in the adult fish [modified from Caputi (Caputi, 1999)]. The activation of the electric organs (EO) in the biphasic larvae (B), in the triphasic larvae (C) and in juveniles and adults (D) is indicated in a schematic based on the adult electrogenic system. Arrows of different colors indicate the different waveform components that are progressively added in the course of postnatal development.

accelerations of the pacemaker mediated by an internal motor collateral (Falconi et al., 1995; Borde et al., 2004). To our knowledge, there are no studies of Mauthner cell-evoked pacemaker acceleration during development of electric fish.

Development of the EOD waveform

The analysis of the electromotive force pattern using the air gap technique allowed us to follow the development of the different EOD waves.

The first wave to appear is V_3, which is caused by the neural activation of the caudal faces of all electrocytes. Following the electrocyte density profile, the tail region shows the largest electrogenic index (i.e. volts/percentage body length). However, despite the similar profile of electrocyte density exhibited by fish of different lengths, the prominence of the electrogenic index at the tail region increases as development progresses. This might result from two structural features. It may come from the different distribution of the ratio between the area of the electrogenic region and the area of the surrounding tissue as observed in Fig. 2A, but it may also be a consequence of the incomplete maturation of the intrinsic properties of the electrocyte membrane of the more caudal regions. In agreement with this hypothesis, we found the presence of immature electrocytes in the tail region. This analysis suggests a rostro-caudal progress of the EO maturation and its electrogenic efficiency.

The second wave to appear is V_4. A small V_4 is sometimes present in the smallest fish but becomes definitively present in fish larger than 20 mm. Similarly to the adult, this wave is completely abolished by partial curarization, confirming that this component is caused by action potentials firing at the rostral faces as a consequence of the propagation of action potentials generating V_3. In addition, the head-to-tail air gap experiments indicate that in larvae the quotient between the peaks of V_4 and V_3 (V_4/V_3) increases between 50 and 100% when the load is changed from 1 MΩ to 1 kΩ. The change of the waveform caused by the load decreases as fish grow (Fig. 7D). This effect indicates that the propagation of the action potentials from the caudal to the rostral faces of electrocytes progressively increases in efficiency from larvae to adults.

In addition, the smaller ratio between the areas of the EO and the surrounding tissues suggests that the internal electric path loading the EO decreases relatively when the fish grow. Thus, the lower efficiency of propagation of the caudal face's action potential observed in small fish is not caused by the lack of internal pathways for the action currents. This suggests that either there is a maturation of the channel repertoire through postnatal life or a folding of the electrocyte membrane increasing the electrogenic area relative to the cross-sectional area of the surrounding tissue.

The early negative waves V_1 and V_2 were analyzed in particular because they reflect the double innervation of a set of electrocytes lying in the latero-dorsal tube of the EO. No head-negative wave preceded V_3 in fish below 20 mm in length. This suggests that either peripheral connectivity is not complete or that the functional coordination of the electromotor neurons' firing is still immature. When it appears, V_1 is generated mainly in the centro-rostral quarter of the fish body. As the fish grows, this generator moves rostrally (Fig. 9) and a second component, the sharp negative wave V_2, appears as a peak in the spatial pattern of electromotive force in fish of about 50 mm length. The different mechanism for V_2 was confirmed by the observation that partial curarization reduces its amplitude more steeply than that of the rostral generator. This is consistent with the accepted hypothesis that V_2 originates in the action potentials fired by the rostral faces of doubly innervated electrocytes (Bennett, 1971; Macadar et al., 1989). This late appearance of V_2 might also indicate a delayed maturation of the channel repertoire of the rostral faces of

electrocytes or, in addition, a delay in the maturation of the spinal and peripheral coordination mechanisms observed in the adult (Caputi and Trujillo-Cenóz, 1994; Caputi and Aguilera, 1996).

Conclusions

The analysis of the EOD timing and waveform as a function of fish length revealed how neural mechanisms involved in the coordination of the different populations of electrogenic units develop, whereas the study of the electromotive force and the total power delivered to water as a function of fish length outlined the development of electrocytic and post effector mechanisms.

The sensorimotor control of the pacemaker rate appears to be complete within the larval stage, as indicated by the statistics of the inter-EOD interval series and by the profile of the novelty responses.

The adult EOD waveform is achieved by adding components according to a consistent sequence (V_3–V_4–V_1–V_2). This sequence reveals that the caudal faces of the electrocytes are the first group of electrogenic elements to be neurally activated, followed by the activation of rostral faces of the more dorsal and lateral tubes in a rostrocaudal sequence (V_1 precedes V_2). Thus, the neural pattern generator appears to be fully mature when fish are about 55 mm in length, which according to the external aspect of the fish could coincide with the transition between late larval and juvenile stages.

While the adult sequence of waveform components appears to be complete at the beginning of the juvenile stage, the total electromotive force increases with length in juveniles, reaching a maximum at about 100 mm in length. The analysis of the electromotive force and the internal resistance of the equivalent generator suggests that during the juvenile stage the electrogenic system increases its output by a dual mechanism: the increase in the electromotive force and the increase in the delivered current.

The increase of electromotive force could be due to two complementary factors. Firstly, the increase in the efficiency of neural synchronization mechanisms, as suggested by the progressive reduction of the duration of the waveform components and the consequent shift of the peak of the power spectra to the higher frequency region. Secondly, the increase in excitability of the electrocyte membrane, as suggested by the increase in the V_4/V_3 ratio when the EO is loaded (Bell et al., 1976).

The increase in delivered current is related to the progressive increase in body length and consequently the reduction of the internal resistance of the equivalent generator (Caputi and Budelli, 1995).

These findings allow us to define three consecutive periods in the development of electrogenesis in this species of *Gymnotus* above 10 mm in length: (1) an early maturation period comprising larval stages during which the neural mechanisms of coordination are able to progressively achieve the tetraphasic sequence characteristic of the species EOD waveform, (2) an intermediate maturation period comprising mainly the juvenile stage during which the electrogenic efficiency increases by maturation of the electrogenic units and (3) a growing period, beyond 100 mm in length, in which the electromotive force stabilizes in amplitude and waveform but the electric power delivered to water continues increasing with fish size.

Two main questions arise from our study: (1) are the rostral faces innervated in fish below 20 mm emitting monophasic pulses, or is there a delayed development of the spinal and peripheral mechanisms coordinating the sequence of activation of electrocyte opposite faces and (2) is there a maturation profile for the electrocyte membrane and its channel repertoire that explains the delayed appearance of V_2 and the increase in efficiency of V_4?

This work was performed in the Department of Integrative and Computational Neurosciences, IIBCE and was partially funded by the following grants: Fogarty # 1R03-TW05680 to PI C. Bell, ECOS U03B01, by NSF grant DEB-0614334 to PI W. Crampton and PEDECIBA. The Faculty of Medicine of the Universidad de la República partially covered the salary of M.E.C. The authors thank Dr Kirsty Grant and Dr Pedro Aguilera for reading and commenting on the manuscript, Carolina Lezcano, Javier Nogueira and María Inés Rehermann for help with the fish collection, Carmen Pereira for fish care, and the Armada Nacional and the Alférez de Navío (CG) Luis Díaz and the personnel from the Naval Base C/C Carlos A. Curbelo for assistance in the exploration of the Cisne Lagoon. Author contributions: A.A.C., experimental design; all authors, experiments; A.R.C., M.E.C. and A.A.C., anatomical analysis; A.R.C., A.C.P., A.A.C., EOD time series analysis; A.C.P. and A.A.C., biophysical analysis; A.A.C., first draft of manuscript.

References

Aguilera, P. A., Castelló, M. E. and Caputi, A. A. (2001). Electroreception in *Gymnotus carapo*: differences between self-generated and conspecific-generated signal carriers. *J. Exp. Biol.* **204**, 185-198.

Albert, J. S. and Crampton, W. (2001). Five new species of *Gymnotus* (Teleostei, Gymnotiformes) from an upper Amazonian floodplain, with description of electric organ discharges and echology. *Ichthyol. Explor. Freshw.* **12**, 241-226.

Albert, J. S. and Crampton, W. (2003). Seven new species of the Neotropical electric fish *Gymnotus* (Teleostei, Gymnotiformes) with a redescription of *G. carapo* (Linnaeus). *Zootaxa* **287**, 1-4.

Albert, J. S. and Crampton, W. (2005). Diversity and Phylogeny of neotropical electric fishes (Gymnotiformes). In *Electroreception* (ed. T. H. Bullock, C. D. Hopkins, A. N. Popper and R. R. Fay), pp. 360-409. New York: Springer.

Baillet-Derbin, C. (1978). Cytodifferentiation of the regenerating electrocyte in an electric fish. *Biol. Cell.* **3**, 15-24.

Bass, A. H. (1986). Electric organs revisited: evolution of the vertebrate communication and orientation organ. In *Electroreception* (ed. T. H. Bullock and W. Heiligenberg), pp. 13-70. New York: Wiley.

Bastian, J. (1986). Electrolocation: behavior, anatomy, and physiology. In *Electroreception* (ed. T. H. Bullock and W. Heiligenberg), pp. 577-612. New York: Wiley.

Bell, C. C., Bradbury, J. and Russell, C. J. (1976). The electric organ of a Mormyrid as a current and voltage source. *J. Comp. Physiol.* **110**, 65-88.

Bennett, M. V. L. (1971). Electric organs. In *Fish Physiology*. Vol. V (ed. W. S. Hoar and D. J. Randall), pp. 347-491. London: Academic Press.

Bennett, M. V. L. and Grundfest, H. (1959). Electrophysiology of electric organ in *Gymnotus carapo*. *J. Gen. Physiol.* **42**, 1067-1104.

Black-Cleworth, P. (1970). The role of electrical discharges in the non-reproductive social behaviour of *Gymnotus carapo* (Gymnotidae, Pisces). *Anim. Behav. Monogr.* **3**, 1-77.

Borde, M., Curti, S., Comas, B. and Rivero, C. (2004). Central modulation of a sensory system by a motor comand. One intention with two results. *Rev. Neurol*. **38**, 253-260.

Bullock, T. H. (1969). Species differences in effect of electroreceptor input on electric organ pacemakers and other aspects of behavior in electric fish. *Brain Behav. Evol.* **2**, 85-118.

Bullock, T. H., Hagiwara, S., Kusano, K. and Negishi, K. (1961). Evidence for a category of electroreceptors in the lateral line of gymnotid fishes. *Science* **134**, 1426-1427.

Caputi, A. A. (1999). The electric organ discharge of pulse gymnotiforms: the transformation of a simple impulse into a complex spatiotemporal electromotor pattern. *J. Exp. Biol.* **202**, 1229-1241.

Caputi, A. and Aguilera, P. (1996). A field potential analysis of the electromotor system in *Gymnotus carapo*. *J. Comp. Physiol. A* **179**, 827-835.

Caputi, A. and Budelli, R. (1995). The electric image in weakly electric fish: I. A data-based model of waveform generation in *Gymnotus carapo*. *J. Comput. Neurosci.* **2**, 131-147.

Caputi, A. A. and Budelli, R. (2006). Peripheral electrosensory imaging by weakly electric fish. *J. Comp. Physiol. A* **192**, 587-600.

Caputi, A. and Trujillo-Cenóz, O. (1994). The spinal cord of *Gymnotus carapo*: the electromotoneurons and their projection patterns. *Brain Behav. Evol.* **44**, 166-174.

Caputi, A., Macadar, O. and Trujillo-Cenóz, O. (1989). Waveform generation of the electric organ discharge in *Gymnotus carapo.* III. Analysis of the fish body as an electric source. *J. Comp. Physiol. A* **165**, 361-370.

Caputi, A., Silva, A. and Macadar, O. (1993). Electric organ activation in *Gymnotus carapo*: spinal origin and peripheral mechanisms. *J. Comp. Physiol. A* **173**, 227-232.

Caputi, A. A., Aguilera, P. A. and Castelló, M. E. (2003). Probability and amplitude of novelty responses as a function of the change in contrast of the reafferent image in *G. carapo*. *J. Exp. Biol.* **206**, 999-1010.

Caputi, A. A., Carlson, B. A. and Macadar, O. (2005). The electric organs and their control. *In Electroreception* (ed. T. H. Bullock, C. D. Hopkins, A. N. Popper and R. R. Fay), pp. 410-452. New York: Springer.

Carlson, B. A. (2002). Electric signaling behavior and the mechanisms of electric organ discharge production in mormyrid fish. *J. Physiol. Paris* **96**, 405-419.

Cox, R. T. and Coates, C. W. (1938). Electrical characteristics of the electric tissue of the electric eel, *Electrophorus electricus* (Linnaeus). *Zoologica* **23**, 203-212.

Crampton, W. and Hopkins, C. D. (2005). Nesting and paternal care in the weakly electric fish *Gymnotus* (Gymnotiformes: Gymnotidae) with descriptions of larval and adult electric organ discharges of two species. *Copeia* **1**, 48-60.

Denizot, J. P., Kirschbaum, F., Westby, G. W. M. and Tsuji, S. (1978). The larval electric organ of the weakly electric fish *Pollimyrus (Marcusenius) isidori* (Mormyridae, Teleostei). *J. Neurocytol.* **7**, 165-181.

Denizot, J. P., Kirschbaum, F., Westby, G. W. M. and Tsuji, S. (1982). On the development of the adult electric organ in the mormyrid fish *Pollimyrus isidori* (with special focus on the innervation). *J. Neurocytol.* **11**, 913-934.

Dye, J. C. and Meyer, J. H. (1986). Central control of the electric organ discharge in weakly electric fish. In *Electroreception* (ed. T. H. Bullock and W. Heiligenberg), pp. 71-102. New York: Wiley.

Eaton, R. C., Farley, R. D., Kimmel, C. B. and Schabtach, E. (1977). Functional development in the Mauthner cell system of embryos and larvae of the zebrafish. *J. Neurobiol.* **8**, 151-172.

Falconi, A., Borde, M., Hernández-Cruz, A. and Morales, F. R. (1995). Mauthner cell initiated abrupt increase of the electric organ dishcarge in the weakly electric fish *Gymnotus carapo*. *J. Comp. Physiol*. *A* **176**, 679-689.

Franchina, C. R. (1997). Ontogeny of the electric organ discharge and the electric organ in the weakly electric pulse fish *Brachyhypopomus pinnicaudatus* (Hypopomidae, Gymnotiformes). *J. Comp. Physiol. A* **181**, 111-119.

Hagedorn, M., Heiligenberg, W. and Carr, C. C. (1988). Development of the jamming avoidance response in the weakly electric fish, *Eigenmannia. Brain Behav. Evol.* **31**, 161-169.

Hagedorn, M., Vischer, H. A. and Heiligenberg, W. (1992). Development of the jamming avoidance response and its morphological correlates in the gymnotiform electric fish, *Eigenmannia*. *J. Neurobiol*. **23**, 1446-1466.

Heiligenberg, W. (1980). The evaluation of the electroreceptive feedback in a gymnotoid fish with pulse-type electric organ discharges. *J. Comp. Physiol. A* **138**, 173-185.

Hopkins, C. D. (1995). Convergent designs for electrogenesis and electroreception. *Curr. Opin. Neurobiol*. **5**, 769-777.

Keynes, R. D., Bennett, M. V. L. and Grundfest, H. (1961). Studies on the morphology and electrophysiology of electric organs. II. Electrophysiology of the electric organ of *Malapterurus electricus*. In *Bioelectrogenesis* (ed. C. Chagas and A. Paes de Carvalho), pp. 102-112. Amsterdam: Elsevier.

Kirschbaum, F. (1977). Electric organ ontogeny distinct larval organ precedes the adult organ in weakly electric fish. *Naturwissenschaften* **7**, 387-388.

Kirschbaum, F. (1983). Myogenic electric organ precedes the neurogenic organ in Apteronotid fish. *Naturwissenschaften* **70**, 205-207.

Kirschbaum, F. and Schugardt, C. (2002). Reproductive strategies and development aspects of mormyrids and gymnotiform fishes. *J. Physiol. Paris* **56**, 557-566.

Kirschbaum, F. and Westby, G. W. M. (1975). Development of electric-discharge in mormyrid and gymnotid fish (*Marcusenius sp and Eigenmannia-virescens*). *Experientia* **31**, 1290-1294.

Knudsen, E. I. (1974). Behavioral thresholds to electric signals in high frequency electric fish. *J. Comp. Physiol*. **91**, 333-353.

Larimer, J. L. and MacDonald, J. A. (1968). Sensory feedback from electroreceptors to electromotor pacemaker centers in gymnotids. *Am. J. Physiol*. **214**, 1253-1261.

Lissmann, H. W. (1958). On the function and evolution of electric organ in fish. *J. Exp. Biol.* **35**, 156-191.

Lorenzo, D., Velluti, J. C. and Macadar, O. (1988). Electrophysiological properties of abdominal electrocytes in the weakly electric fish *Gymnotus carapo*. *J. Comp. Physiol. A* **162**, 141-144.

Macadar, O. (1993). Motor control of waveform generation in *Gymnotus carapo. J. Comp. Physiol*. *A* **173**, 728-729.

Macadar, O., Lorenzo, D. and Velluti, J. C. (1989). Waveform generation of the electric organ discharge in *Gymnotus carapo*. II. Electrophysiological properties of single electrocytes. *J. Comp. Physiol. A* **165**, 352-360.

Meyer, J. H. (1982). Behavioral responses of weakly electric fish to complex impedances. *J. Comp. Physiol.* **145**, 459-470.

Moller, P. (1995). *Electric Fishes: History and Behavior*. London: Chapman and Hall.

Ramón y Cajal, S. and De Castro, F. (1933). Elementos de técnica micrográfica del sistema nervioso. Barcelona, Madrid, Buenos Aires: Salvat Editores.

Schuster, S. and Otto, N. (2002). Sensitivity to novel feedback at different phases of a gymnotid electric organ discharge. *J. Exp. Biol.* **205**, 3307-3320.

Srivastava, C. B. L. and Baillet-Derbin, C. (1973). Etude ultraestructurale de l'organe électrique d'un poisson électrique à faible décharge: eigenmania virescens. *C. R. Acad. Sci. Paris* **277**, 2209-2212.

Srivastava, C. B. L. and Szabo, T. (1972). Development of electric organs of *Gymnarchus niloticus* (Fam Gymnachidae) I. Origin and histogenesis of electroplates. *J. Morphol.* **138**, 375-385.

Szabo, T. (1960). Development of the electric organ of Mormyridae. *Nature* **188**, 760-762.

Szabo, T. and Fessard, A. (1965). Le fontionnement des électrorécepteurs étudié chez le Mormyres. *J. Physiol. Paris* **57**, 343-360.

Trujillo-Cenóz, O. and Echagüe, J. A. (1989). Waveform generation of the electric organ discharge in *Gymnotus carapo* I. Morphology and innervation of the electric organ. *J. Comp. Physiol. A* **165**, 343-351.

Trujillo-Cenóz, O., Echagüe, J. A. and Macadar, O. (1984). Innervation pattern and electric organ discharge waveform in *Gymnotus carapo* teleostei Gymnotiformes. *J. Neurobiol*. **15**, 273-281.

Trujillo-Cenóz, O., Echagüe, J. A., Bertolotto, C. and Lorenzo, D. (1986). Some aspects of the structural organization of the spinal cord of Gymnotus carapo (Teleostei, Gymnotiformes). I. The electromotor neurons. *J. Ultrastruct. Mol. Struct. Res.* **97**, 130-143.

Viete, S. and Heiligenberg, W. (1991). The development of the jamming avoidance response (JAR) in *Eigenmannia*: an innate behavior indeed. *J. Comp. Physiol. A* **169**, 15-23.

Zakon, H. H. and Unguez, G. A. (1999). Development and regeneration of the electric organ. *J. Exp. Biol.* **202**, 1427-1434.

Zakon, H., McAnelly, L., Smith, G. T., Dunlap, K., Lopreato, G., Oestreich, J. and Few, W. P. (1999). Plasticity of the electric organ discharge: implications for the regulation of ionic currents. *J. Exp. Biol.* **202**, 1409-1416.